Reduction of tubulin expression in *Angomonas deanei* by RNAi modifies the ultrastructure of the trypanosomatid protozoan and impairs division of its endosymbiotic bacterium

Carolina Moura Costa Catta-Preta[a,c,d], Bruno dos Santos Pascoalino[b], Wanderley de Souza[a], Jeremy C. Mottram[c,d], Maria Cristina M. Motta[a1] & Sergio Schenkman[b1]

[a] Laboratório de Ultraestrutura Celular Hertha Meyer, Instituto de Biofísica Carlos Chagas Filho, Universidade Federal do Rio de Janeiro, Rio de Janeiro, RJ, Brasil.

[b] Escola Paulista de Medicina, Universidade Federal de São Paulo, São Paulo, Brasil.

[c] Wellcome Trust Centre for Molecular Parasitology, Institute of Infection, Immunity and Inflammation, College of Medical, Veterinary and Life Sciences, University of Glasgow, Glasgow, G12 8TA, UK

[d]Centre for Immunology and Infection, Department of Biology, University of York, York, YO10 5DD, United Kingdom.

Keywords: *Angomonas deanei*; endosymbiont; RNAi; cytoskeleton; tubulin; cell division.

[1] Correspondence:

M.C.M. Motta, Laboratório de Ultraestrutura Celular Hertha Meyer, Instituto de Biofísica Carlos Chagas Filho, Universidade Federal do Rio de Janeiro, Av. Carlos Chagas Filho, 373, bloco G subsolo, Cidade Universitária, Rio de Janeiro 21949-900, Brazil
Telephone number: +55-21-39386580; FAX number: +55-21-22602364; E-mail: motta@biof.ufrj.br; and S. Schenkman, Department of Microbiology, Immunology and Parasitology, Escola Paulista de Medicina, Universidade Federal de São Paulo, R. Pedro de Toledo 669, 04039-032 São Paulo, SP Brazil; Telephone number: +55-11-55764870; Email: sschenkman@unifesp.br

Running head: RNAi in a symbiont-bearing trypanosomatid

ABSTRACT

In the last two decades, RNA interference pathways have been employed as a useful tool for reverse genetics in trypanosomatids. *Angomonas deanei* is a non-pathogenic trypanosomatid that maintains an obligatory endosymbiosis with a bacterium related to the Alcaligenaceae family. Studies of this symbiosis can help us to understand the origin of eukaryotic organelles. The recent elucidation of both the *A. deanei* and the bacterium symbiont genomes revealed that the host protozoan codes for the enzymes necessary for RNAi activity in trypanosomatids. Here we tested the functionality of the RNAi machinery by transfecting cells with dsRNA to a reporter gene (green fluorescent protein), which had been previously expressed in the parasite and to α-tubulin, an endogenous gene. In both cases, protein expression was reduced by the presence of specific dsRNA, inducing, respectively, a decreased GFP fluorescence and the formation of enlarged cells with modified arrangement of subpellicular microtubules. Furthermore, symbiont division was impaired. These results indicate that the RNAi system is active in *A. deanei* and can be used to further explore gene function in symbiont-containing trypanosomatids and to clarify important aspects of symbiosis and cell evolution.

Trypanosomatids are widely studied protozoa because they cause diseases with high rates of mortality among low-income population of Africa, Asia and Americas (WHO 2012). Several genetic tools have been developed to study the biology of trypanosomatids, aiming to better understand the mechanisms involved in the establishment of infection. Among them, RNA interference (RNAi) can be used to reduce gene expression. RNAi was initially described in *Trypanosoma brucei* electroporated with double-stranded RNA (dsRNA) corresponding to α-tubulin genes (Ngo et al. 1998). It was reported that this dsRNA decreased α-tubulin expression and disrupted the cell structure to produce enlarged protozoa that were called FAT cells, most likely due to an unbalanced production of α and β-tubulin dimers (Ngo et al. 1998). Tubulin dimers form the structure of microtubule arrays found underneath the plasma membrane and are essential to shape trypanosomatids (De Souza 1988). Later, the RNAi pathway was confirmed by the identification of endogenous non-encoding RNA, known as small interfering RNA (Djikeng et al. 2001). The presence of Argonaute (Ago1) and two Dicer-like (Dcl1 and Dcl2) genes homologues, which encode the classical RNAi machinery and are required for the decrease in gene expression, were then identified in the *T. brucei* genome and their functions were established experimentally (Durand-Dubief and Bastin 2003, Shi et al. 2004, Shi et al. 2006, Patrick et al. 2009). Altogether, these findings made RNAi the methodology of choice for studies on the cell biology and gene expression of *T. brucei*, leading to rapid progress in understanding the biology of this parasite (Kolev et al. 2011).

RNAi is also present in some Leishmania species such as *L. braziliensis,* which also contains the expected RNAi machinery. Indeed, gene expression was specifically decreased in strains expressing stem-loop RNA complementary to endogenous and

reporter genes (Lye et al. 2010). However, some trypanosomatids such as *Trypanosoma cruzi*, *Leishmania major* and *Leishmania donovani* lack the genes and the activities related to RNAi, or contain degenerate machinery that is not active, as in *Trypanosoma rangeli* (Stoco et al. 2014).

Many trypanosomatids, however, do not cause disease in mammals, but are valuable models to study trypanosomatid biology and their life cycle, as well as for the understanding of the evolutionary origin of eukaryotic cells. *Angomonas deanei* is a trypanosomatid that has a mutualistic relationship with a symbiotic bacterium (Alves et al. 2011). It offers a rare opportunity to comprehend how obligatory endosymbionts can give rise to organelles, such as mitochondria and plastids (Motta 2010). Recently, the genomes of *A. deanei* and its symbiont were sequenced (Motta et al. 2013). This opened the possibility to better understand the molecular mechanisms that regulate symbiosis in trypanosomatids, such as the control of cell division and the metabolic exchanges between partners. Among the genes of *A. deanei,* we found the presence of homologues of Ago1 and a Dicer, also identified in other monoxenous species such as *Crithidia fasciculata* and *Leptomonas seymouri* (Kraeva et al. 2015, Lye et al. 2010). Therefore, here we tested whether the RNAi machinery is active in *A. deanei*. For this, we analyzed the effects of introducing a synthetically prepared dsRNA corresponding to α-tubulin into *A. deanei.* We observed modifications in the subpellicular microtubule arrangement, as well as impairment in division of the symbiotic bacterium. We also found that dsRNA corresponding to the green fluorescent protein (GFP) gene was able to decrease its expression in *A. deanei* stably transfected with GFP. These results indicate that the RNAi machinery is functional in *A. deanei,* since reduction of tubulin expression generated cells with a modified arrangement of subpellicular microtubules and symbiont

filamentation, indicating blockage of the bacterium division. These findings open perspectives to use monoxenous and non-pathogenic trypanosomatids for studies of gene expression, and also to gain insights into the role of different proteins related to the maintenance of the symbiosis.

MATERIAL AND METHODS

Bioinformatic analysis

RNAi machinery enzymes were identified during the annotation of *A. deanei* proteins, based on what was previously described for other trypanosomatids, by using the BLAST tool of SABIA (System for Automated Bacterial Integrated Annotation) (Almeida et al. 2004, Motta et al. 2013). Identified sequences were submitted to domain searches against Pfam (Finn et al. 2014) and Interpro (Hunter et al. 2012) databases to confirm the putative sequence functions. Conserved domains of Ago1 and Dicer-like proteins were aligned with their respective trypanosomatids ortholog proteins by using MUSCLE software (Edgar 2004). To generate the phylogenetic trees, we used Clustal alignment and PhyML (Guindon et al. 2010) available through the Geneious 8.0 package (http://www.geneious.com).

Protozoan cultivation

A. deanei was isolated from *Zelus leucogrammus* in 1973 by A.L.M. Carvalho (ATCC 30255) and was maintained at 28°C in Warren's culture medium (Warren 1960) supplemented with 10% fetal calf serum (South American Origin from, Thermo Fisher Scientific, São Paulo, Brazil). Experiments were performed with exponentially growing cells maintained for 24 h in the culture medium.

dsRNA synthesis and transfection

Sense and antisense RNA strands were synthesized from linearized DNA templates containing T7 and SP6 promoters, using the RiboMAX™ T7 and SP6 Large Scale RNA Production System (Promega, Madison, WI, USA). The DNA sequences coding for the N- and C-terminal regions of *A. deanei* α-tubulin (ATMG01003360) were obtained by PCR using the primers OL1 and OL2, or OL3 and OL4 (Table S1). GFP was amplified from the plasmid pRockGFPNeo (DaRocha et al. 2004) by using primers OL5 and OL6. The amplified fragments were purified after electrophoresis in agarose gel in Tris-Acetate EDTA buffer by using the QIAquick Gel Extraction Kit (Qiagen, Valencia, CA, USA). Fragments were cloned in pGEM-T Easy Vector (Promega). For the transcription reactions, plasmids were digested with *Nco*I and *Nde*I for the synthesis with T7 and SP6 RNA polymerases, respectively. After transcription and digestion of the DNA templates with RNase-free DNase (Roche Life Sciences, Indianapolis, IN, USA), the produced RNAs were submitted to electrophoresis in agarose gels, purified by using the QIAquick Gel Extraction Kit (Qiagen), and quantified with NanoDrop 2000c (Thermo Scientific). dsRNA was generated as described (Ngo et al. 1998).

Electroporation was performed with 10^8 cells in 0.4 ml electroporation buffer (21 mM Hepes, 137 mM NaCl, 5 mM KCl, 0.7 mM NaH_2PO_4 and 6 mM glucose) by using the program U-033 of the Amaxa Nucleofactor (Lonza, Allendale, NJ, USA). In order to avoid RNA degradation, dsRNA was added to the indicated concentrations immediately before the transfection. Controls were performed with cells transfected with annealed RNA, transcribed using the non-specific (Mock) DNA control, provided by the transcription kit. To determine the ideal incubation time and dsRNA concentration to induce phenotypic changes, we counted 500 cells of each time point and concentration.

Statistical analysis was performed using the GraphPad Prism 5.0 software (San Diego, CA, USA). Two-way ANOVA was performed and p values < 0.05 were considered significant. Bonferroni post-tests were performed after two-way ANOVA for multiple samples analysis using the GraphPad Prism 5.0 software.

Generation of *A. deanei* strain expressing α-tubulin-GFP

A. deanei strain expressing a heterologous fluorescent protein was obtained using the vector pMOTag3G GFP (Oberholzer et al. 2006) to tag *A. deanei* α-tubulin. This vector allows the expression of a protein fused to a tag at the same levels of the endogenous wild-type gene *via* a one-step PCR-mediated transfection procedure that introduces the tag *in situ*. Vector construction was performed as described (Oberholzer et al. 2006) using the primers OL7 and OL8. The PCR product was pooled and precipitated with isopropanol, washed once with ethanol, dried and resuspended in TE buffer. Transfection was made as described for dsRNA. Control was performed using the non-amplified vector. Cells were selected for G418 resistance (50 μg/ml) and cloned by limiting dilution after 3 days. This drug concentration was selected by a previous titration and was found to be the minimal concentration that prevented cell growth. After 7 days the clones were checked by epifluorescence and flow cytometry and the brighter ones were selected.

Immunofluorescence

Cells were washed in PBS, deposited on poly-L-lysine-coated slides, and fixed in -20 °C methanol for 20 min. The slides were incubated 1 h in blocking solution containing 1.5% BSA, 0.5% teleostean gelatin and 0.02% Tween 20 in PBS (pH 8.0). This was followed by 1 h incubation with the following antibodies diluted in blocking solution: 1:2 anti-symbiont porin (Andrade et al. 2011), 1:50 MAb acetylated tubulin (Sigma-

Aldrich, St. Louis, MI, USA), 1:50 monoclonal antibody anti-α-tubulin (EP1332Y from Abcam, Cambridge, UK) and 1:100 anti-GFP (Thermo Fisher Scientific). After washing with PBS, cells were further incubated for 45 min with secondary antibodies such as Alexa 488, or 555, IgG anti-rabbit, or anti-mouse, depending on the primary antibody. Slides were mounted in Prolong Gold containing 4', 6-diamidino-2-phenylindole (DAPI, from Molecular Probes, Thermo Fisher). Serial image stacks (0.2-μm Z-increment) were collected at 100x, oil immersion, 1.4 NA, on a motorized Olympus BX microscope equipped with differential interference contrast optics, and an Orca R2 camera (Hamamatsu Photonics K.K. Hamamatsu City, Japan). All images were collected with Cell^M software (Olympus America Incorporation, Center Valley, PA, USA), and fluorescence images were deconvolved with the AutoQuant 2.2 software by using blind deconvolution (Media Cybernetics Inc. Rockville, MD, USA). For comparative reasons, we always used the same exposure times during slides analysis. Alternatively, samples were visualized with confocal laser scanning microscope (Zeiss LSM510 META from Carl Zeiss, Jena, Germany). Projection of the Z-axis and the 3D reconstructions were obtained and processed using the Z-stack systems of the microscope software.

Electron microscopy

For electron transmission microscopy, cells were washed in PBS and fixed with 2.5% glutaraldehyde in 0.1 M cacodylate buffer, pH 7.2, for 1 h. After washing again in 0.1 M cacodylate buffer, pH 7.2, cells where post-fixed for 1 h in 1% osmium tetroxide containing 0.8% potassium ferrocyanide, 5 mM $CaCl_2$ in 0.1 M cacodylate buffer. Next, cells were washed, dehydrated in several crescent concentrations of acetone and embedded in Epon; first a mix of Epon:acetone (1:1) and finally in pure Epon (Electron Microscopy Sciences, Hatfield, PA, USA). Ultrathin sections were obtained using an

Ultracut Reichert Ultramicrotome and mounted on 400-mesh copper grids, and then were stained with uranyl acetate and lead citrate. Samples were analyzed in a Tecnai Spirit (FEI, Hillsboro, OR, USA). For scanning electron microscopy protozoa were adhered to 0,1% poly-L-lysine-covered cover slips, fixed and post fixed as described above. Then, cells were submitted to dehydration in ascending ethanol series, critical point-dried with CO_2 in a CPD 030 critical point dryer (Balzers, Liechtenstein, Germany), sputtered with gold in a FL-9496 sputter coater (Balzers) and observed using a Quanta 250 digital scanning microscope (FEI). Cells were measured with the help of Image J (Abramoff et al. 2004).

Cytometry analysis

Parasites expressing GFP were analyzed in an Accuri C6 cytometer (BD Bioscience, Franklin Lakes, NJ, USA) in order to verify GFP expression for clone selection and after 1, 6 and 12 h of electroporation with dsRNA complementary to GFP. For this purpose, aliquots of 250 μl were removed from the culture, washed and resuspended in electroporation buffer. Fluorescence was measured using FL1 filter after counting 50,000 events. Data analysis was performed in BD Accuri software.

Western blotting

Protein levels in control and dsRNA-electroporated cells were analyzed by Western blotting. In cells electroporated with α-tubulin dsRNA, differential centrifugations were performed at 1,000 g for 5 min, in order to obtain an enriched population of cells presenting abnormal morphology (FAT phenotype). Each lane was loaded with 1 x 10^6 cells and SDS-PAGE and Western blotting was performed as described before (Andrade et al. 2011). Anti-α-tubulin (1:5000), anti-acetylated tubulin (1:500) and anti-actin (MAb Anti-β-Actin - clone AC-74 1, Sigma-Aldrich) were used to

identify differences in protein expression after α-tubulin or GFP dsRNA transfection. Actin was used as a loading control. Immunolabeling with anti-actin antibody was performed in membranes previously submitted to anti-α-tubulin or anti-GFP labeling after stripping with a commercially available buffer (Thermo Fisher Scientific). Cells (1 x 10^6), which were electroporated with GFP-dsRNA, as well as WT control-cells, were submitted to the same procedure described above and incubated with a 1:500 dilution of anti-GFP (Molecular Probes, USA). Densitometry analysis was performed using Image J (Abramoff et al. 2004).

Real time PCR

Cells transfected as described for dsRNA were either harvested for total population analysis or enriched for FAT cells as described bellow. The RNA was prepared using the RNeasy kit (Qiagen). First strand cDNA was prepared using 4 μg of RNA for each sample using the First strand synthesis kit (Thermo Fisher Scientific). The cDNA was treated with RNase H (Thermo Fisher Scientific) to degrade the template RNA. The PCR reactions were set using SYBR green PCR master mix (Applied Biosystems, Foster City, CA, USA) using oligonucleotides OL9 and OL10 for amplifying the N-terminal region of *A. deanei* tubulin. Actin (OL11 and OL12) or GAPDH (OL13 and OL14) were used as an endogenous control. The qPCR was run and analyzed on a 7300 Real time PCR system (Applied Biosystems).

RESULTS

***A. deanei* contains conserved Ago and Dicer-like genes**

Genes encoding proteins that are part of the RNAi machinery, such as Ago1 and Dicer, were previously identified in the genome of *A. deanei* (Motta et al. 2013). *A. deanei*

argonaute protein Ago1 had a higher level of identity with PAZ (32.3%) and Piwi (35.5%) domains of *C. fasciculata* than *T. brucei* (27% and 29%, respectively) and *L. braziliensis* (31% and 33%, respectively), (Fig. 1A and S1A and S1B). *A. deanei* dicer-like protein Dcl1 contains a well conserved RNAse III single domain, as observed in *T. brucei*, while in *L. braziliensis* and *C. fasciculata* Dcl1 has 2 domains (Fig. 1B). *A. deanei* RNAse III domain was more related to the *T. brucei* than to the *L. braziliensis* and *C. fasciculata* sequences (Fig. S1C).

The protein characteristics of Ago1 and Dcl1 are conserved in *L. braziliensis* and *C. fasciculata* (Lye et al. 2010), as well as in species of *Trypanosoma*. *A. deanei* genes diverged more from other trypanosomatid species, as suggested by the phylogenetic analyses for both full length Ago1 and Dicer-like amino acid sequences and in the alignment of each domain separately (Fig. 1C-D and S1). However, bootstrap supports are rather low and further analysis with additional species should be performed to evaluate the evolutionary origin of these proteins in this group of organisms.

dsRNA causes depletion on expression of a reporter gene

Next, we decided to test whether the RNAi machinery is active by transfecting *A. deanei* with dsRNA transcribed and annealed *in vitro* to induce easily recognized phenotypes. Therefore, we targeted cells expressing α-tubulin fused with GFP with dsRNA of the GFP coding sequence. Tagged cells were prepared by transfection with a PCR fragment containing the 3' region of α-tubulin fused to GFP obtained by amplification of the pMOTAG-3G vector, which is normally used for epitope tagging *of T. brucei* (Oberholzer et al. 2006). The *A. deanei* were then selected with G418 and cloned to obtain a homogeneous cell population expressing GFP. We found that immunofluorescence labeling with anti-α-tubulin and anti-GFP antibodies co-localized

(Fig. 2A), indicating that the correct gene locus was targeted. No fluorescence was observed in non-transfected cells (Fig. S2). These cells were then subjected to transfection with 50 μg/ml dsRNA complementary to the GFP. After 1 h, live cells had a 10-fold decrease in GFP fluorescence, as detected by flow cytometry (Fig. 2B). After 6 h in culture, the fluorescence levels were reduced to almost to background levels. In accordance with these data, immunofluorescence labeling using anti-α-tubulin and anti-GFP antibodies also decreased after transfection (Fig. 2A).

Quantitative analysis was further performed by Western blot, confirming that dsRNA disrupted the expression of the fusion protein 6 h after transfection (Fig. 2C). Because the GFP was expressed as fusion protein with tubulin, we also examined the levels of the endogenous tubulin in those cells using α-tubulin antibody. As shown in figure 1C, the endogenous tubulin did not decrease.

dsRNA to α-tubulin causes changes in the shape of symbiont and bacteria filamentation

To further confirm that dsRNA was affecting gene expression we targeted endogenous α-tubulin mRNA, with the expectation that this would lead to a FAT-like phenotype as previously observed for *T. brucei* (Ngô et al. 1998). Wild type cultures were transfected with 10 to 100 μg/ml dsRNA corresponding to the sequences encoding the N- or C-terminal regions of α-tubulin. The cell morphology was observed by differential interference contrast microscopy and immunofluorescence analysis during the first 24 h, which corresponds to four-generation times in *A. deanei* (Motta 2010). dsRNA at concentrations below 25 μg/ml did not affected the cells, which remained similar to control parasites (Fig. 3A). Enlarged cells were observed at 50 μg/ml (Fig. 3B)

and their number increased with higher dsRNA concentration (75 and 100 μg/ml), or longer times after electroporation (Fig. 3C and D). When using 100 μg/mL dsRNA (the highest concentration tested), the number of enlarged (FAT) cells increased up to 16% after 24 h of transfection. No enlarged cells were observed in the non-transfected controls, or controls transfected without non-relevant (GFP, in this case) dsDNA (Fig. 3D). When compared to untransfected cells, enlarged cells also contained a larger nucleus and a single kinetoplast. In addition, several cells were found to contain the symbiotic bacterium in a filamentous state, which is an abnormal phenotype that only occurs when bacteria are not able to divide (see dotted lines in Fig. 3B and C; Movie S1).

We found that the tubulin mRNA levels of cells transfected with 50 μg/ml dsRNA of the N-terminus of α-tubulin decreased progressively by 18% compared to water, or mock transfected cells from 6 to 24 h after transfection (Fig. 3E), which indicates that α-tubulin mRNAs were degraded in the total population. This small but significant decrease ($p<0.05$) was determined in three independent experiments and was similar when using dsRNA corresponding to the C-terminus fragment. In these analyses, actin and GAPDH were used as controls and mRNA remained constant in treated and non-treated samples. We then quantified RNA for α-tubulin in a population enriched for enlarged cells collected by low speed centrifugation 24 h after transfection. In this case, a progressive degradation of tubulin mRNA was observed with a maximum of 94% reduction in mRNA observed after 24 h (Fig. 3E).

As seen by Western blots, the levels of α-tubulin also decreased up to 65% (n=3) with increasing concentrations of α-tubulin relative to actin (Fig 3F). No decrease in α-tubulin levels was observed when we used a non-specific dsRNA (M) as a control,

indicating that this decrease in expression was specific and the FAT phenotype was related to a decreased expression of α-tubulin.

We confirmed the filamentous nature of the symbiotic bacterium and block in cytokinesis of the enlarged protozoan cells by staining the bacterium with DAPI and with a specific anti-porin antibody that labeled the bacterial envelope and facilitated the fission visualization (Fig. 4A). Quantitative analysis of these images revealed that about 90% of the enlarged cells contained long symbiont filaments (Fig. 4B)

We also found a similar decrease in tubulin expression by using anti-acetylated tubulin antibodies, which are known to label stable subpellicular microtubules (Souto-Padron et al. 1993) (Fig. 5A). Immunofluorescence analyses confirmed that cells transfected with dsRNA of α-tubulin contained a filamentous symbiont and a cytoskeleton with subpellicular microtubules that seemed to be more spaced from each other in relation to control cells (Fig. 5B). These results support a direct correlation between dsRNA transfection and the observed FAT cell phenotype.

ds-tubulin RNA causes alterations in microtubule elements

Scanning electron microscopy showed that, in contrast to control cells (Fig. 6A), cells transfected with dsRNA of α-tubulin had an atypical morphology, sometimes lacking a flagellum emerging from the flagellar pocket (Fig. 6B). While transmission electron microscopy of control cells revealed well-defined cytoplasmic distribution of organelles (Fig. 6C), an evident disorganization of subcellular structures was found in cells transfected with dsRNA, including filamentation of the bacterial symbiont (Fig. 6D, arrow). In comparison to control cells (Fig. 6E and 6F), we observed a more spaced distribution of the subpellicular microtubules (Fig. 6G). This was observed in 50 control and transfected cells. While in control cells a regular space of 50 nm was found, in

transfected cells we detected an irregular space varying from 15 to 95 nm. We also noticed the lack of the central pair of microtubules in the flagellum axoneme in some cells (Fig. 6H), which is in accordance with the reduced expression of α-tubulin. The above images were obtained using dsRNA for the N-terminal α-tubulin, but similar observations were made with the dsRNA corresponding to the C-terminal of α-tubulin, which also generated FAT cells. More importantly, similar results were also obtained when C and N-terminal of β-tubulin were used separately as the degradation target (data not shown).

DISCUSSION

Here, we confirmed the presence of the dicer and argonaute-like genes involved in the RNAi pathway and demonstrated that cell transfection with double strand RNA affected specific gene expression in *A. deanei*. Our analyses showed that the sequences present in *A. deanei* encode for proteins with RNAseIII domains of dicer and Paz and Piwi of argonaute similar to the ones found in *T. brucei*, *L. braziliensis,* and several monoxenous species such as *C. fasciculata* and *L. seymouri.* Unfortunately, it was not possible to evaluate the evolutionary origins of these genes based on synteny analysis, since the *A. deanei* genome has not been assembled. Our phylogenetic results suggested that both enzymes could have evolved from a common ancestor of *Trypanosoma* and *Leishmania/Crithidia* branches, although more analyses are required. Nevertheless, this is an interesting feature, since *A. deanei* is phylogenetic closer to the *Leishmania* genus than to *Trypanosoma* (Motta et al. 2013), forming with *Kentomonas* sp a new group of trypanosomatids with endosymbionts (Votypka et al. 2014). Our findings agree with the

fact that *A. deanei* also contains genes for the RNA interference factor (RIF) 4 and 5, known to directly interact with Ago1 in *T. brucei* (Barnes et al. 2012).

The effectiveness of RNAi in *A. deanei* was demonstrated after transfecting cells with dsRNA corresponding to α-tubulin sequences, since it decreased expression, caused changes in the cell morphology, and affected the host and the symbiont division. The morphology was apparently changed by the reduction in the α-tubulin content, similarly to what was shown for *T. brucei* (Ngo et al. 1998). A hallmark in symbiont bearing trypanosomatids ultrastructure is the typical microtubule arrangement, where subpellicular microtubules are absent in regions in which branches of the mitochondrion touch the plasma membrane (Faria e Silva et al. 1991). Therefore, it was expected that reduction in α-tubulin expression would parallel the redistribution of subpellicular microtubules, which indeed became more spaced and irregular in FAT cells. In addition, the absence of an external flagellum in cells displaying the FAT phenotype could be related to the lack of the microtubule central pair on the axoneme, as observed by transmission electron microscopy. These are similar to the phenotypes observed in in *T. brucei* with tubulin RNAi, in which cytoskeleton structures, such as microtubules of the Flagellum Attachment Zone and the subpellicular microtubules, were affected (Ngo et al. 1998).

Only a relatively small proportion of *A. deanei* underwent the transformation to FAT cells, which parallels the decrease in α-tubulin expression. This might be due to poor transfection efficiency in relation to *T. brucei*, although it is comparable to other trypanosomatids. Importantly, in all enlarged cells a specific decrease of tubulin was detected; indicating that at least in this population the transfection with dsRNA was effectively inducing inhibition of expression.

The fact that cells enlarged and contained an augmented nucleus suggested that cell division was also arrested. Probably, the depletion of tubulin affected the formation of mitotic spindles, thus blocking cell division. More interesting in this case is that the knockdown of α-tubulin lead to symbiont filamentation, which is in agreement with our previous studies showing that the symbiont division is coordinated with the host nucleus (Motta 2010). Moreover, compounds that specifically arrest the protozoan cell cycle, as well as tubulin polymerization caused symbiont filamentation (Catta-Preta et al. 2015). These results further confirmed our hypothesis that the host cell cytoskeleton plays a role in the endosymbiont division, which may represent a way to control the number of bacteria.

We also demonstrated for the first time that *A. deanei* can be genetically manipulated. The cells were able to incorporate, probably by homologous recombination, a DNA segment containing an α-tubulin-GFP fusion and the neomycin gene that conferred resistance to Geneticin G418, as described in *T. brucei* (Oberholzer et al. 2006). The recovery and selection occurred in 3 days, when 87% of cells in the culture were fluorescent. Individual clones were obtained 7 days after limiting dilution, which is compatible with the fast doubling time of *A. deanei*. The presence of GFP-fusion, detectable by anti-GFP and anti-tubulin in Western Blotting, suggested the appropriate insertion of the gene in the tubulin locus, instead of being expressed through an episome. Importantly, the exogenous inserted GFP sequence was also a specific target for RNAi with a significant reduction in expression after the first hours in culture. The dsGFP did not cause the FAT phenotype because the endogenous tubulin levels were not decreased, further supporting the specificity of the RNAi process. Interestingly, we observed an increase in the endogenous tubulin after depletion of the GFP-tubulin

fusion. Perhaps, this increase occurred because the expression of the tubulin in fusion with GFP reduced the tubulin expression. As the fusion protein is depleted by the RNAi using GFP sequences, the endogenous levels of tubulin increased, further confirming targeting specificity.

In conclusion, our results provide strong evidence that *A. deanei* is an RNAi proficient trypanosomatid. The RNAi in *A. deanei* can be exploited to understand the evolutionary pathways of this silencing machinery and, due the presence of a bacterial symbiont, to answer questions related to eukaryotic cell evolution, helping to understand the molecular mechanisms involved in symbiosis maintenance, symbiont division control and metabolism interdependence (Motta et al. 2013, Alves et al. 2013, Klein et al. 2013, Azevedo-Martins et al. 2015).

ACKNOWLEDGEMENTS

This work was supported by Grants from the Conselho Nacional de Desenvolvimento Científico e Tecnológico (CNPq), Fundação de Amparo à Pesquisa do Estado do Rio de Janeiro (FAPERJ), Fundação de Amparo à Pesquisa do Estado de São Paulo (FAPESP, 2011/51973-3) and the Medical Research Council (MR/K019384).

LITERATURE CITED

Abramoff, M. D., Magelhaes, P. J. & Ram, S. J. 2004. Image Processing with ImageJ. *Biophotonics Int.,* 11**:**36-42.

Almeida, L. G., Paixao, R., Souza, R. C., Costa, G. C., Barrientos, F. J., Santos, M. T., Almeida, D. F. & Vasconcelos, A. T. 2004. A System for Automated Bacterial (genome) Integrated Annotation--SABIA. *Bioinformatics,* 20**:**2832-3.

Alves, J. M., Voegtly, L., Matveyev, A. V., Lara, A. M., da Silva, F. M., Serrano, M. G., Buck, G. A., Teixeira, M. M. & Camargo, E. P. 2011. Identification and phylogenetic analysis of heme synthesis genes in trypanosomatids and their bacterial endosymbionts. *PLoS One,* 6**:**e23518.

Alves, J. M., Klein, C. C., da Silva, F. M., Costa-Martins, A. G., Serrano, M. G., Buck, G. A., Vasconcelos, A. T., Sagot, M. F., Teixeira, M. M., Motta, M. C. & Camargo, E. P. 2013. Endosymbiosis in trypanosomatids: the genomic cooperation between bacterium and host in the synthesis of essential amino acids is heavily influenced by multiple horizontal gene transfers. *BMC Evol. Biol.,* 13**:**190.

Andrade, I. d. S., Vianez-Junior, J. L., Goulart, C. L., Homble, F., Ruysschaert, J. M., Almeida von Kruger, W. M., Bisch, P. M., de Souza, W., Mohana-Borges, R. & Motta, M. C. 2011. Characterization of a porin channel in the endosymbiont of the trypanosomatid protozoan *Crithidia deanei*. *Microbiology,* 157**:**2818-30.

Azevedo-Martins, A. C., Machado, A. C., Klein, C. C., Ciapina, L., Gonzaga, L., Vasconcelos, A. T., Sagot, M. F., W, D. E. S., Einicker-Lamas, M., Galina, A. & Motta, M. C. 2015. Mitochondrial respiration and genomic analysis provide insight into the influence of the symbiotic bacterium on host trypanosomatid oxygen consumption. *Parasitol.,* 142**:**352-62.

Barnes, R. L., Shi, H., Kolev, N. G., Tschudi, C. & Ullu, E. 2012. Comparative genomics reveals two novel RNAi factors in *Trypanosoma brucei* and provides insight into the core machinery. *PloS Pathog.,* 8**:**e1002678.

Catta-Preta, C. M., Brum, F. L., da Silva, C. C., Zuma, A. A., Elias, M. C., de Souza, W., Schenkman, S. & Motta, M. C. 2015. Endosymbiosis in trypanosomatid protozoa: the bacterium division is controlled during the host cell cycle. *Front. Microbiol.,* 6**:**520.

DaRocha, W. D., Silva, R. A., Bartholomeu, D. C., Pires, S. F., Freitas, J. M., Macedo, A. M., Vazquez, M. P., Levin, M. J. & Teixeira, S. M. 2004. Expression of exogenous genes in *Trypanosoma cruzi*: improving vectors and electroporation protocols. *Parasitol. Res.,* 92**:**113-20.

De Souza, W. 1988. The cytoskeleton of trypanosomatids. *Mem. Inst. Oswaldo Cruz,* 83 Suppl 1**:**546-560.

Djikeng, A., Shi, H., Tschudi, C. & Ullu, E. 2001. RNA interference in *Trypanosoma brucei*: cloning of small interfering RNAs provides evidence for retroposon-derived 24-26-nucleotide RNAs. *RNA,* 7**:**1522-30.

Durand-Dubief, M. & Bastin, P. 2003. TbAGO1, an argonaute protein required for RNA interference, is involved in mitosis and chromosome segregation in *Trypanosoma brucei*. *BMC Biol.,* 1**:**2.

Edgar, R. C. 2004. MUSCLE: multiple sequence alignment with high accuracy and high throughput. *Nucleic Acids Res.,* 32**:**1792-7.

Faria e Silva, P. M., Sole-Cava, A. M., Soares, M. J., Motta, M. C., Fiorini, J. E. & de Souza, W. 1991. *Herpetomonas roitmani* (Fiorini et al., 1989) n. comb.: a trypanosomatid with a bacterium-like endosymbiont in the cytoplasm. *J. Protozool.,* 38**:**489-94.

Finn, R. D., Bateman, A., Clements, J., Coggill, P., Eberhardt, R. Y., Eddy, S. R., Heger, A., Hetherington, K., Holm, L., Mistry, J., Sonnhammer, E. L., Tate, J. & Punta, M. 2014. Pfam: the protein families database. *Nucleic Acids Res.,* 42**:**D222-30.

Guindon, S., Dufayard, J. F., Lefort, V., Anisimova, M., Hordijk, W. & Gascuel, O. 2010. New algorithms and methods to estimate maximum-likelihood phylogenies: assessing the performance of PhyML 3.0. *System Biology,* 59**:**307-21.

Hunter, S., Jones, P., Mitchell, A., Apweiler, R., Attwood, T. K., Bateman, A., Bernard, T., Binns, D., Bork, P., Burge, S., de Castro, E., Coggill, P., Corbett, M., Das, U., Daugherty, L., Duquenne, L., Finn, R. D., Fraser, M., Gough, J., Haft, D., Hulo, N., Kahn, D., Kelly, E., Letunic, I., Lonsdale, D., Lopez, R., Madera, M., Maslen, J.,

McAnulla, C., McDowall, J., McMenamin, C., Mi, H., Mutowo-Muellenet, P., Mulder, N., Natale, D., Orengo, C., Pesseat, S., Punta, M., Quinn, A. F., Rivoire, C., Sangrador-Vegas, A., Selengut, J. D., Sigrist, C. J., Scheremetjew, M., Tate, J., Thimmajanarthanan, M., Thomas, P. D., Wu, C. H., Yeats, C. & Yong, S. Y. 2012. InterPro in 2011: new developments in the family and domain prediction database. *Nucleic Acids Res.,* 40**:**D306-12.

Klein, C. C., Alves, J. M., Serrano, M. G., Buck, G. A., Vasconcelos, A. T., Sagot, M. F., Teixeira, M. M., Camargo, E. P. & Motta, M. C. 2013. Biosynthesis of vitamins and cofactors in bacterium-harbouring trypanosomatids depends on the symbiotic association as revealed by genomic analyses. *PLoS One,* 8**:**e79786.

Kolev, N. G., Tschudi, C. & Ullu, E. 2011. RNA interference in protozoan parasites: achievements and challenges. *Eukariot. Cell,* 10**:**1156-63.

Kraeva, N., Butenko, A., Hlavacova, J., Kostygov, A., Myskova, J., Grybchuk, D., Lestinova, T., Votypka, J., Volf, P., Opperdoes, F., Flegontov, P., Lukes, J. & Yurchenko, V. 2015. *Leptomonas seymouri*: Adaptations to the Dixenous Life Cycle Analyzed by Genome Sequencing, Transcriptome Profiling and Co-infection with *Leishmania donovani*. *PloS Pathog.,* 11**:**e1005127.

Lye, L. F., Owens, K., Shi, H., Murta, S. M., Vieira, A. C., Turco, S. J., Tschudi, C., Ullu, E. & Beverley, S. M. 2010. Retention and loss of RNA interference pathways in trypanosomatid protozoans. *PloS Pathog.,* 6**:**e1001161.

Motta, M. C. 2010. Endosymbiosis in trypanosomatids as a model to study cell evolution. *Open Parastitol. J.,* 4**:**139-147.

Motta, M. C., Martins, A. C., de Souza, S. S., Catta-Preta, C. M., Silva, R., Klein, C. C., de Almeida, L. G., de Lima Cunha, O., Ciapina, L. P., Brocchi, M., Colabardini, A. C., de Araujo Lima, B., Machado, C. R., de Almeida Soares, C. M., Probst, C. M., de Menezes, C. B., Thompson, C. E., Bartholomeu, D. C., Gradia, D. F., Pavoni, D. P., Grisard, E. C., Fantinatti-Garboggini, F., Marchini, F. K., Rodrigues-Luiz, G. F., Wagner, G., Goldman, G. H., Fietto, J. L., Elias, M. C., Goldman, M. H., Sagot, M. F., Pereira, M., Stoco, P. H., de Mendonca-Neto, R. P., Teixeira, S. M., Maciel, T. E., de Oliveira Mendes, T. A., Urmenyi, T. P., de Souza, W., Schenkman, S. & de Vasconcelos, A. T. 2013. Predicting the Proteins of *Angomonas deanei*, *Strigomonas culicis* and Their Respective Endosymbionts Reveals New Aspects of the Trypanosomatidae Family. *PLoS One,* 8**:**e60209.

Ngo, H., Tschudi, C., Gull, K. & Ullu, E. 1998. Double-stranded RNA induces mRNA degradation in *Trypanosoma brucei*. *Proc. Natl. Acad. Sci. USA,* 95**:**14687-14692.

Oberholzer, M., Morand, S., Kunz, S. & Seebeck, T. 2006. A vector series for rapid PCR-mediated C-terminal in situ tagging of *Trypanosoma brucei* genes. *Mol. Biochem. Parasitol.,* 145**:**117-20.

Patrick, K. L., Shi, H., Kolev, N. G., Ersfeld, K., Tschudi, C. & Ullu, E. 2009. Distinct and overlapping roles for two Dicer-like proteins in the RNA interference pathways of the ancient eukaryote *Trypanosoma brucei*. *Proc. Natl. Acad. Sci. USA,* 106**:**17933-8.

Shi, H., Tschudi, C. & Ullu, E. 2006. An unusual Dicer-like1 protein fuels the RNA interference pathway in *Trypanosoma brucei*. *RNA,* 12**:**2063-72.

Shi, H., Ullu, E. & Tschudi, C. 2004. Function of the *Trypanosome* Argonaute 1 protein in RNA interference requires the N-terminal RGG domain and arginine 735 in the Piwi domain. *J. Biol. Chem.,* 279**:**49889-49893.

Souto-Padron, T., Cunha e Silva, N. L. & de Souza, W. 1993. Acetylated alpha-tubulin in Trypanosoma cruzi : immunocytochemical localization. *Mem. Inst. Oswaldo Cruz,* 88**:**517-528.

Stoco, P. H., Wagner, G., Talavera-Lopez, C., Gerber, A., Zaha, A., Thompson, C. E., Bartholomeu, D. C., Luckemeyer, D. D., Bahia, D., Loreto, E., Prestes, E. B., Lima, F. M., Rodrigues-Luiz, G., Vallejo, G. A., Filho, J. F., Schenkman, S., Monteiro, K. M., Tyler, K. M., de Almeida, L. G., Ortiz, M. F., Chiurillo, M. A., de Moraes, M. H., Cunha Ode, L., Mendonca-Neto, R., Silva, R., Teixeira, S. M., Murta, S. M., Sincero, T. C., Mendes, T. A., Urmenyi, T. P., Silva, V. G., DaRocha, W. D., Andersson, B., Romanha, A. J., Steindel, M., de Vasconcelos, A. T. & Grisard, E. C. 2014. Genome of the avirulent human-infective trypanosome -*Trypanosoma rangeli*. *PLoS Negl. Trop. Dis.,* 8**:**e3176.

Votypka, J., Kostygov, A. Y., Kraeva, N., Grybchuk-Ieremenko, A., Tesarova, M., Grybchuk, D., Lukes, J. & Yurchenko, V. 2014. *Kentomonas* gen. n., a new genus of endosymbiont-containing trypanosomatids of Strigomonadinae subfam. n. *Protist,* 165**:**825-38.

Warren, L. G. 1960. Metabolism of *Schizotrypanum cruzi* Chagas. I. Effect of culture age and substrate concentration on respiratory rate. *J. Parasitol.,* 46**:**529-39.

WHO 2012. Research priorities for Chagas disease, human African trypanosomiasis and leishmaniasis. *World Health Organization technical report series,* v-xii**:**1-100.

Figures

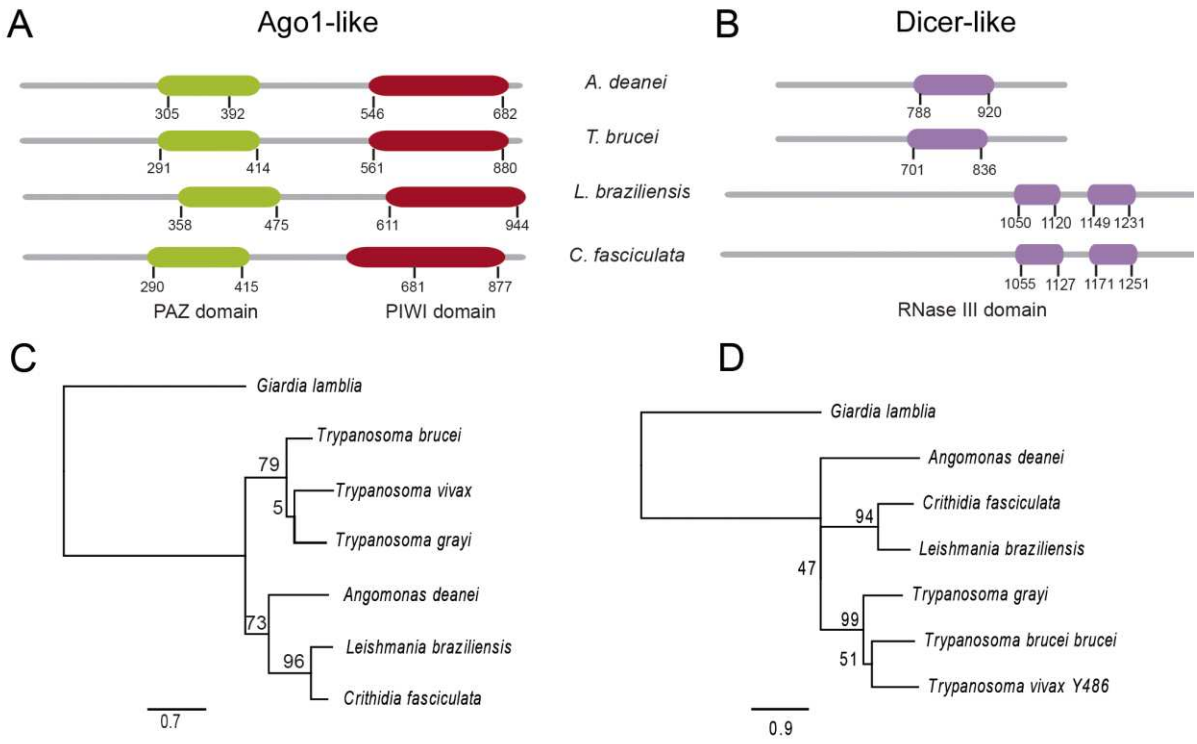

Figure 1 The putative domains of Argonaute (Ago1-like) and Dicer-like are conserved in trypanosomatids. **A** and **B** show respectively the Ago1 and Dicer-like protein alignments generated by Muscle. The Dicer-like proteins are from *A. deanei* (Genbank 21542), *T. brucei* (Genbank XP_847070), *C. fasciculata* (Tritryp CfaC1_31_0570), and *L. braziliensis* (Genbank XP_001565111) and the alignment of the argonaute-like genes are from *A. deanei* (Genbank EPY26085), *T. brucei* (Tritryp Tb927.8.2370), *C. fasciculata* (Tritryp CfaC1_22_0600), and *L. braziliensis* (Genbank EPY26085). The highlights correspond respectively to the RNAse III domains and the PAZ and Piwi-like domains for Dicer-like and PAZ/Piwi-like domains. **C** and **D** show the corresponding phylogenetic trees of Argonaute and Dicer like proteins. In addition to the sequences listed above, it included the sequences of *Giardia lamblia* (Genbank DCL_GIAIC), *T. vivax* (Genbank CCC49571) and *T. grayi* (Tritryp Tgr.139.1090-1) for Dicer-like proteins and the sequences from *G. lamblia* (Genbank AGO_GIAIC), *T. vivax* (Genbank CCC52015) and *T. grayi* (Genbank XP_009312127) for Ago1 related sequences. *G. lamblia* were used as out-group sequences. The numbers in the tree are bootstrap values using 4 substitutions rates and 100 bootstraps and fast topology search. The distance is represented as a horizontal bar at the bottom.

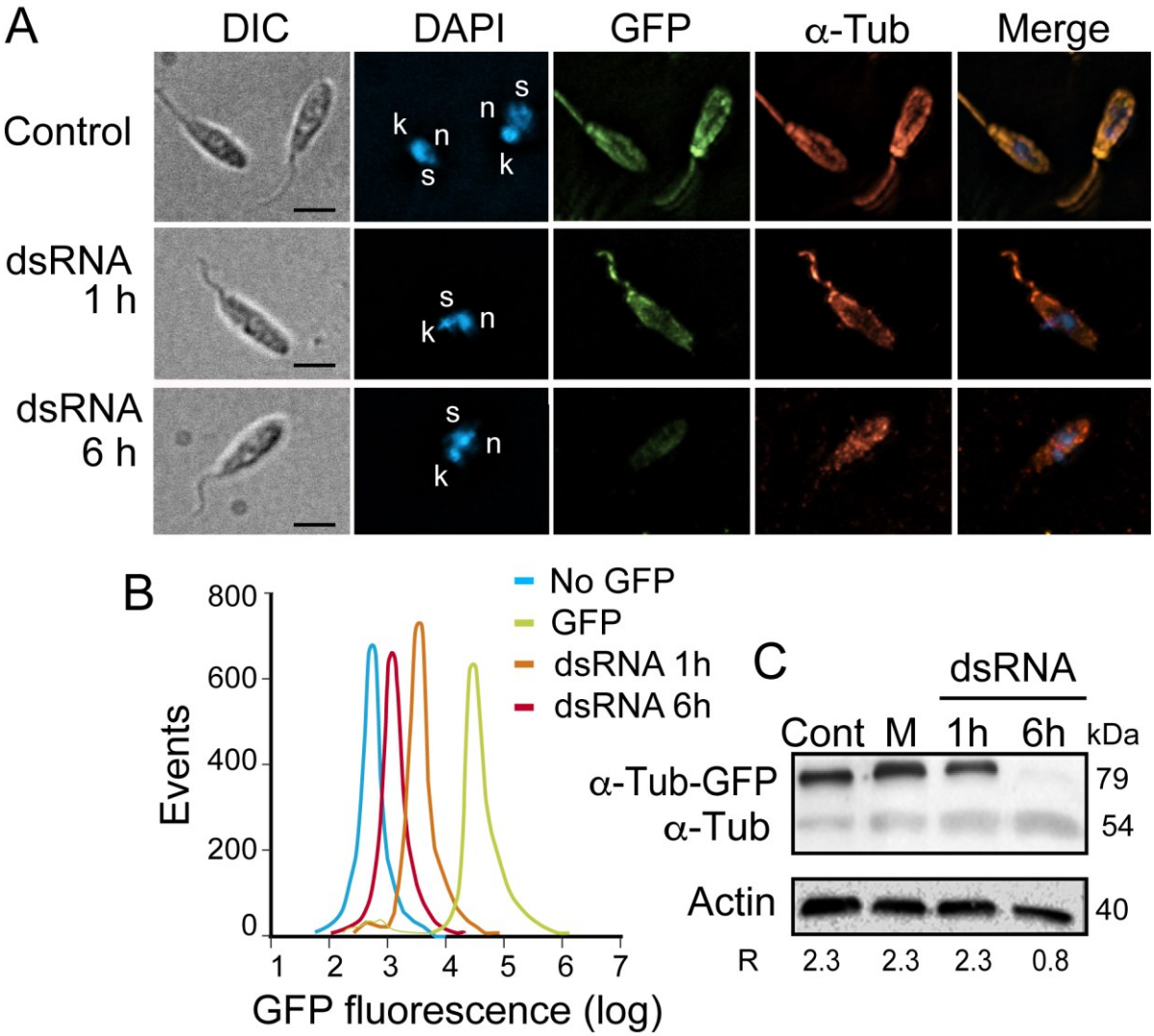

Figure 2 Reporter gene silencing can be triggered by dsRNA. (**A**) Immunofluorescence analysis of cells expressing α-tubulin-GFP (pMOTag 3G α-tubulin) before (Control), 6 h after mock transfection (M), and 1 h or 6 h after transfection with 50 µg/ml of dsRNA of GFP sequences. (**B**) GFP fluorescence of live cells observed by flow cytometry in cells without GFP (blue line), in cells expressing the α-tubulin-GFP fusion (green line), or the same cells 1 h (orange line) or 6 h after transfection (red). The fluorescent content of α-tubulin-GFP cells was maintained for at least 5 days. (**C**) Western blotting of pMOTag 3G α-tubulin cells (Cont), of the same cells 1 h after dsRNA transfection (1 h), or 6 h after transfection (6 h). The membranes were probed with anti-α-tubulin (top panel) and actin antibodies (bottom panel).

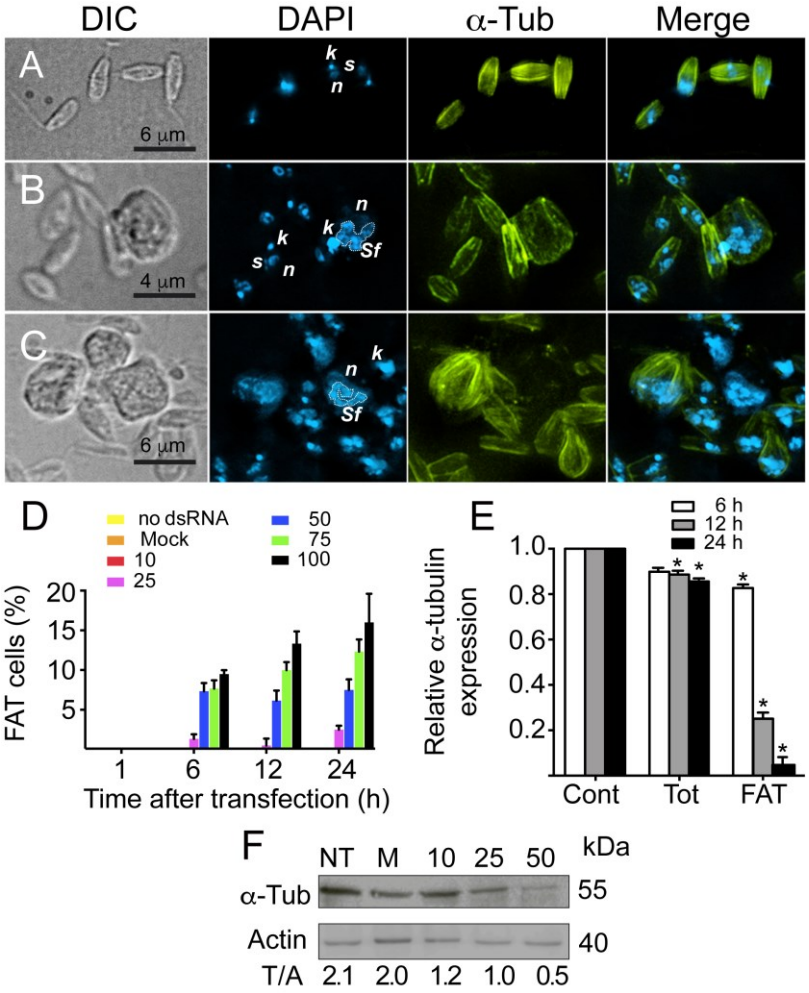

Figure 3 Effect of tubulin dsRNA on *A. deanei*. Exponentially growing *A. deanei* were directly processed for immunofluorescence (**A**) or processed after 24 h of the transfection with 50 µg/ml dsRNA corresponding to the 5' coding region of the α-tubulin gene (**B** and **C**). The slides were incubated with anti-α-tubulin antibodies and stained using anti-rabbit IgG Alexa 488 and DAPI. The images were taken by using differential interference contrast (DIC) or by the appropriate fluorescence filters. S, symbiont; Sf, filamentous symbiont (dotted line); k, kinetoplast, and n, nucleus. Panel (**D**) shows the numbers of FAT cells found 24 h after transfection with the indicated concentrations of dsRNA in µg/ml. Panel (**E**) shows a qPCR analysis of total *A. deanei* RNA isolated at the indicated times after the mock transfection (Contl) or the transfection with dsRNA for the N-terminus of α-tubulin using the entire cell population (Tot) or FAT-enriched cells (FAT). The values shown in **D** and **E** are mean ± standard deviation (n=3). Asterisks indicate significant results when compared to the control ($p < 0.05$). Panel (**F**) shows a Western blot of samples taken from non-transfected *A. deanei* (NT), or 24 h after transfection with mock RNA (M), or with 10, 25 or 50 µg/ml of dsRNA as indicated. The numbers below indicate the mean ratio between the α-tubulin and actin signals (T/A) of three independent experiments.

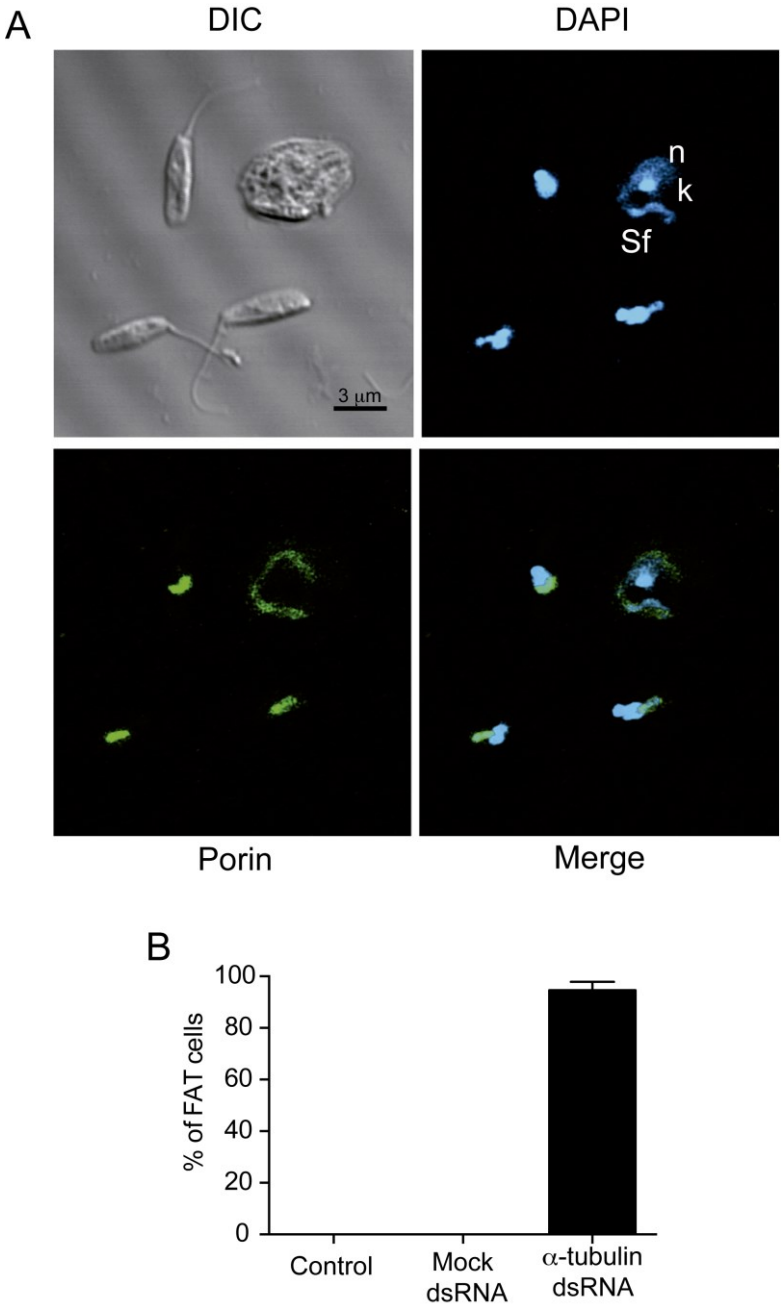

Figure 4 The endosymbiont becomes filamentous in *A. deanei* transfected with α-tubulin dsRNA. Protozoa were transfected with α-tubulin dsRNA and after 24 h processed for immunofluorescence using anti-porin antibodies. Panel **A** shows the DIC, DAPI and the immunofluorescence images. Panel **B** shows the percentage ± standard deviation of FAT cells containing filamentous symbionts in non-transfected (Control), mock transfected and cells transfected with 50 μg/ml of α-tubulin dsRNA (n = 250).

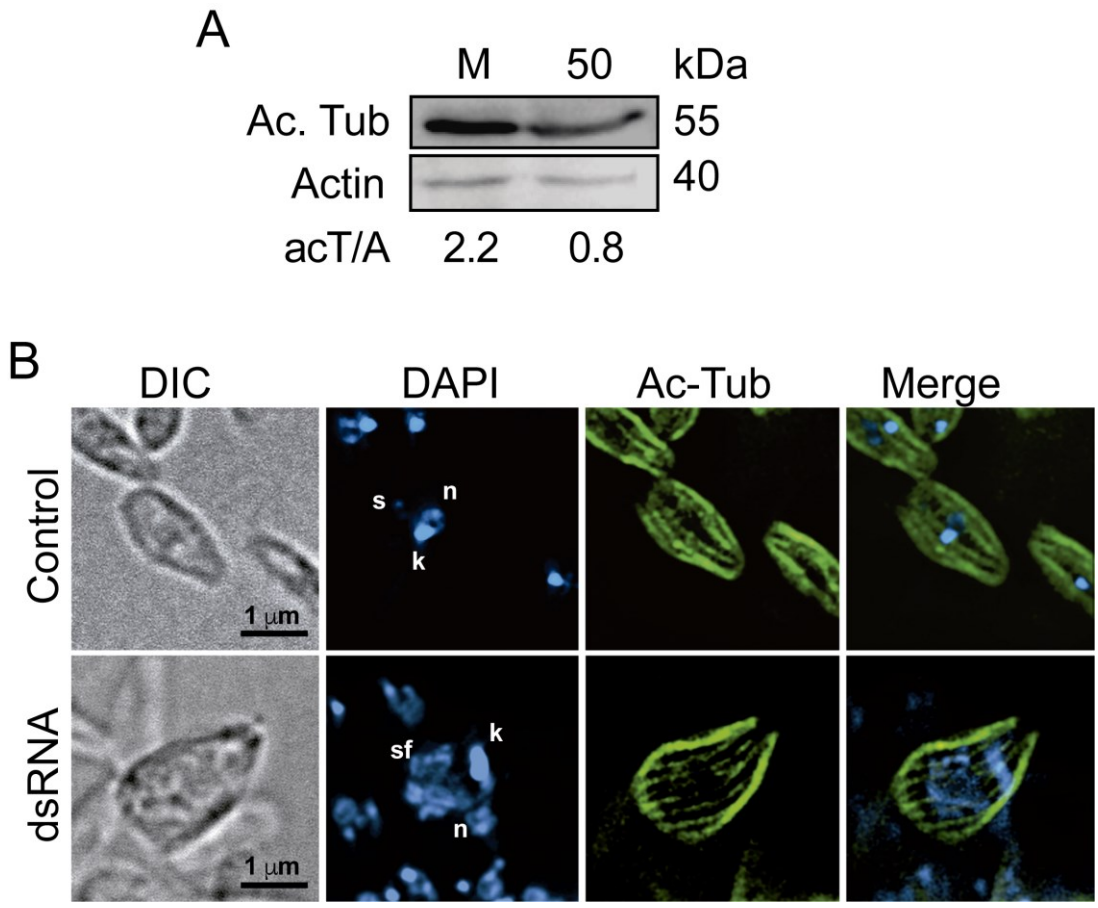

Figure 5 *A. deanei* transfected with α-tubulin dsRNA produced more spaced microtubule arrays. Mock-transfected cells (M) or cells transfected with 50 μg/ml α-tubulin dsRNA (50) were maintained in culture for 24 h and then processed for Western Blot (**A**) by using anti-acetylated tubulin and anti-Actin antibodies. The numbers below the lanes represent the ratio between acetylated-tubulin and actin (Ac-T/A). The same cells were also processed for immunofluorescence (**B**) by using anti-acetylated tubulin antibodies and DAPI staining. S, symbiont, Sf - symbiont , k - kinetoplast, n - nucleus.

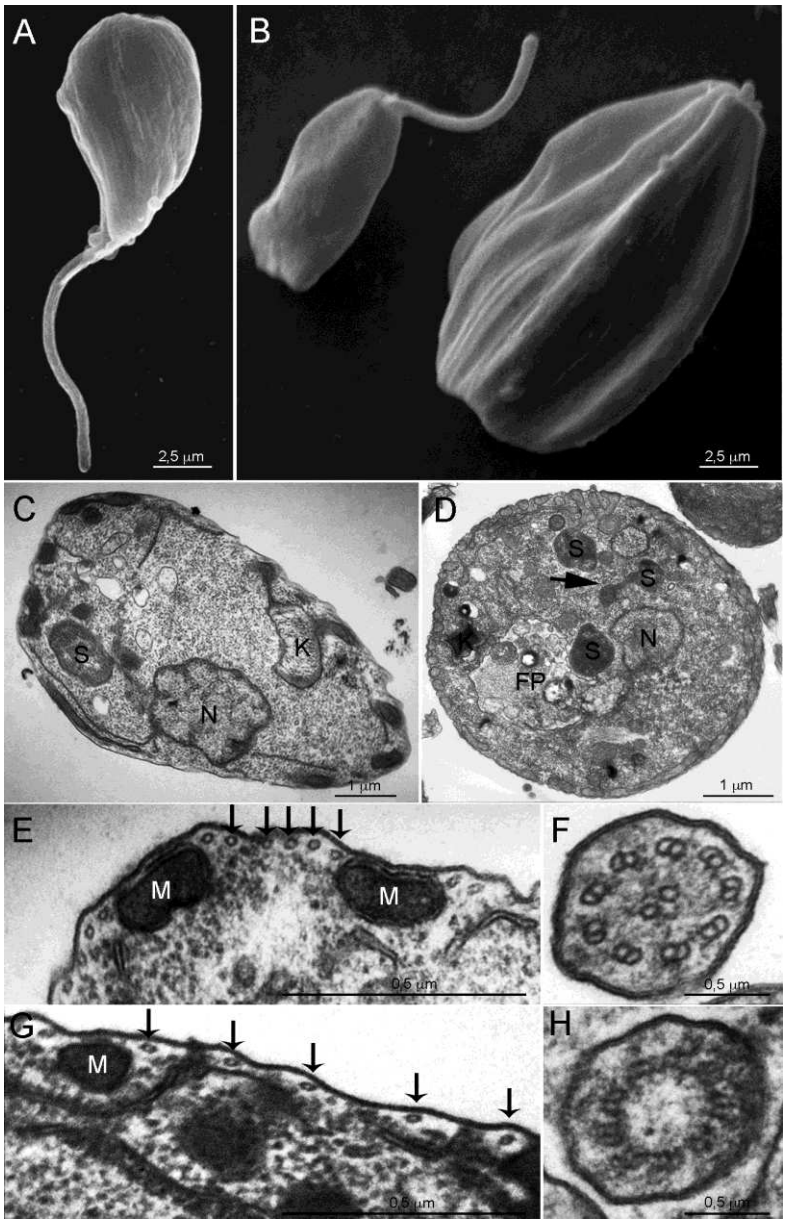

Figure 6 Ultrastructural analysis of *A. deanei* subjected to α-tubulin dsRNA transfection. The figures shows control cells (**A**, **C**-**E**) or cells transfected with 50 μg/ml of α-tubulin dsRNA maintained in culture for 24 h (**B** and **D**, **F**-**H**). The preparations were processed for scanning electron microscopy (**A**-**B**) and transmission electron microscopy (**C**-**H**). The symbiont in control cells is always observed next to the nucleus (**C**). Transfected cells with FAT phenotype displayed cytoplasmic disorganization and multiple symbiont profiles (see arrow), supporting the notion that the bacterium is filamentous (**D**). The subpellicular microtubules (arrows) presented a more spaced and irregular distribution (**G**) in comparison to control cells (**E**). The central pair of microtubules was absent in some of the FAT phenotype cells (**H**), as observed when compared to control cells (**F**) FS- filamentous symbiont, M- mitochondrial branches, N- nucleus, FP – flagellar pocket. Scale bars are indicated in the images.

Supplementary information

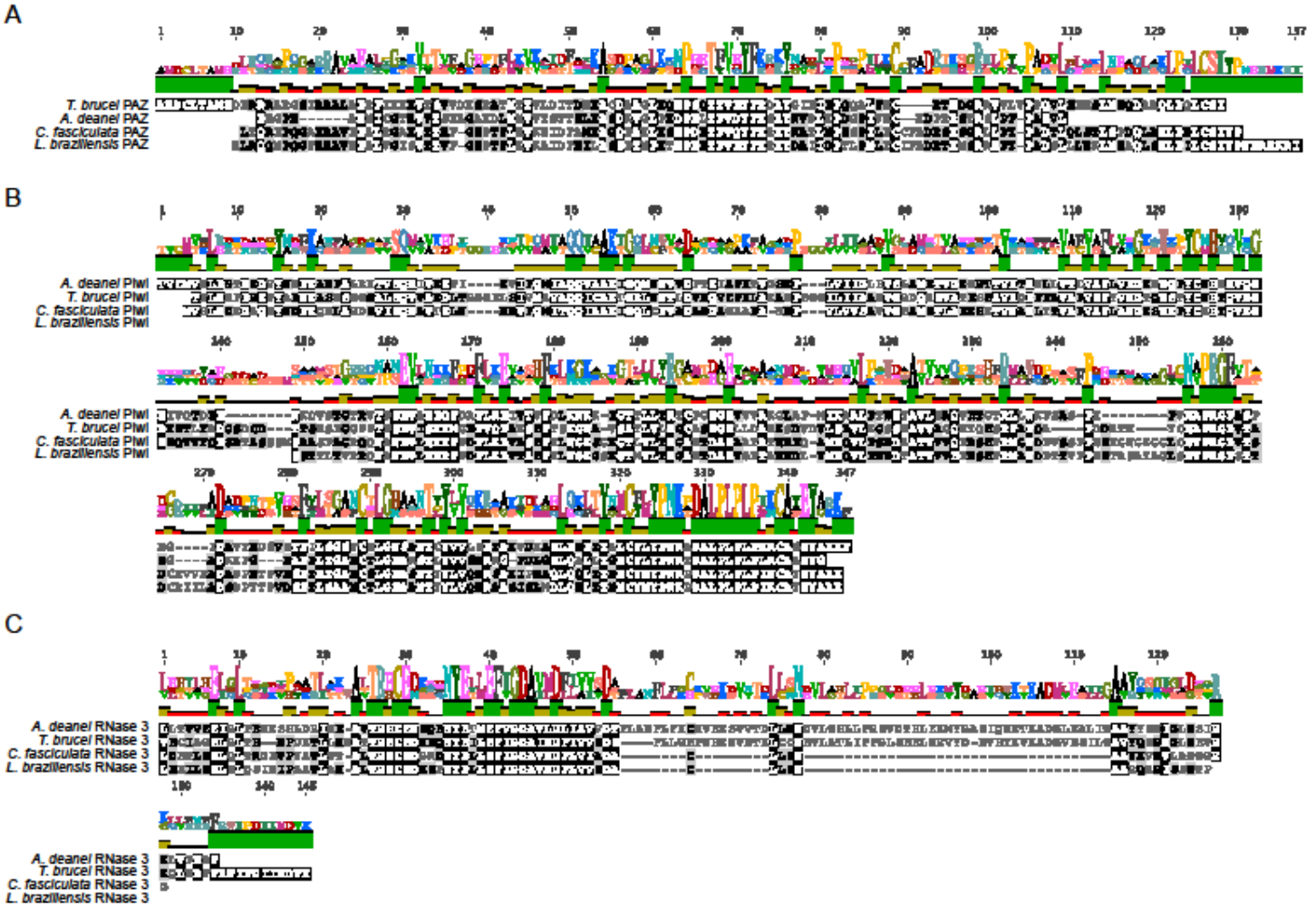

Figure S1 – Muscle alignment of Ago1 (A-B) and Dicer (C) domain sequences.

Figure S2 - *A. deanei* shows no GFP fluorescence. The figure shows a typical cell labeleled with anti-α-tubulin antibodies and observed by DIC, DAPI staining, or fluorescences settings Alexa 488 and Alexa 594 filters. Bar = 2 μm.

Supplementary Table I - Oligonucleotides used in this work

Oligonucleotide	Sequence	Use
OL1	5’CAGGCCGGTTGCCAGGTTG	α-Tub N-term Foward
OL2	5’CTCCTTACCGGAGATGAGCTGC	α-Tub N-term Reverse
OL3	5’CATCAAGACGAAGCGCAC	α-Tub C-term Foward
OL4	5’CTCGGAGAACTCGCCTTCC	α-Tub C-term Reverse
OL5	5’AAGCTTATGAGTAAAGGAGAAG	GFP Fow
OL6	5’GGATCCGTATAGTTCATCCATGCC	GFP Rev
OL7	5’GAACGACCTCGTCTCCGAGTACCAGCAGTACC AGGACGCCACCGTCGAGGAGGAGGGTGAGTTCG ACGAAGAGGAGGAGGGATACGGTACCGGGCCCC CCCTCGAG	In situ tagging Fow
OL8	5’GGGTAGAAAACATTCTTACAGGAATACGCTTA AACATTTCAACGGTGTTAAAGTTGACAAACATG CGCGTAAGACCGACATCCGTTGGCGGCCGCTCT AGAACTAGTGGAT	In situ tagging Rev
OL9	5'-GGAGACCAGTGCAGTTATCG	qPCR tubulin Fow
OL10	5'- CACCAACTCCGTCTTCGAG	qPCR tubulin Rev
OL11	5'-AAGCGTGGTGTGCTTTCC	qPCR actin Fow
OL12	5' GTTCGTTGTAGAAGGTGTGGTG	qPCR actin Rev
OL13	5' ATCATCCCCAGTACCACTGG	qPCR GAPDH Fow
OL14	5' GACATGCCGGTGAGCTTAC	qPCR GAPDH Rev